Improving breast cancer outcome by preoperative systemic therapy and image-guided surgery

Mieog, J.S.D.

Chapter 9

Image-guided tumor resection using real-time near-infrared fluorescence in a syngeneic rat model of primary breast cancer

Mieog JSD, Hutteman M, van der Vorst JR, Kuppen PJK, Que I, Dijkstra J, Kaijzel EL, Prins F, Löwik CWGM, Smit VTHBM, van de Velde CJH, Vahrmeijer AL

ABSTRACT

Introduction

Tumor involvement of resection margins is found in a large proportion of patients who undergo breast-conserving surgery. Near-infrared (NIR) fluorescence imaging is an experimental technique to visualize cancer cells during surgery.

Methods

To determine the accuracy of real-time NIR fluorescence imaging in obtaining tumor-free resection margins, a protease-activatable NIR fluorescence probe and an intraoperative camera system were used in the EMR86 orthotopic syngeneic breast cancer rat model.

Results

Influence of concentration, timing and number of tumor cells were tested in the MCR86 rat breast cancer cell line. These variables were significantly associated with NIR fluorescence probe activation. Dosing and tumor size were also significantly associated with fluorescence intensity in the EMR86 rat model, whereas time of imaging was not. Real-time NIR fluorescence guidance of tumor resection resulted in a complete resection of 17 out of 17 tumors with minimal excision of normal healthy tissue (mean minimum and a mean maximum tumor-free margin of 0.2 ± 0.2 mm and 1.3 ± 0.6 mm, respectively). Moreover, the technique enabled identification of remnant tumor tissue in the surgical cavity. Histological analysis revealed that the NIR fluorescence signal was highest at the invasive tumor border and in the stromal compartment of the tumor.

Conclusion

NIR fluorescence detection of breast tumor margins was successful in a rat model. The present study suggests that clinical introduction of intraoperative NIR fluorescence imaging has the potential to increase the number of complete tumor resections in breast cancer patients undergoing breast-conserving surgery.

INTRODUCTION

Incomplete tumor resections are an important clinical problem in breast cancer surgery. Tumor involvement of resection margins is found in 5-40% of patients who undergo breast-conserving surgery and these patients require additional surgery or intensified radiotherapy.[1-4] Furthermore, additional biopsies of the surgical cavity after primary resection have been shown to contain residual disease in 10% of patients with tumor-free specimen margins.[5] As a result, 5-year isolated local recurrences rates of 6.7-11% are reported in patients with tumor-free specimen margins treated with breast-conserving surgery and radiotherapy.[6] The occurrence of local relapse reduces the 15-year breast cancer specific and overall survival.[6] Consequently, increase of the radical resection rate will likely improve breast cancer outcome. Intraoperative real-time visualization of cancer cells is a promising method to achieve that goal.[7]

Near-infrared (NIR) fluorescence imaging is an experimental technique that can be used to visualize cancer cells during surgery. In current surgical practice, surgeons can only rely on palpation and visual inspection. Therefore, the use of NIR fluorescence imaging can be of great value, as already demonstrated in patients with glioma and liver cancer.[8-10] Advantages of NIR fluorescence light (700-900nm) include high tissue penetration (up to several centimeters deep) and low autofluorescence providing sufficient signal-to-background ratio.[11] Moreover, as the human eye is insensitive to NIR wavelengths, the use of NIR light will not interfere with the surgical field.

NIR fluorescence probes can target tumor cells through several mechanisms. For example, fluorophores can be conjugated to a tumor-specific antibody (e.g. directed to the Her-2/neu receptor), labeled to glucose derivates in order to visualize elevated metabolic rate, or autoquenched fluorophores can be activated by enzymatic cleavage in order to become fluorescent. The latter is of particular interest as certain enzyme systems are upregulated by a wide variety of cancer types, thus providing a more universally applicable NIR fluorescence probe. Proteolytic enzymes and in particular cathepsins from the cysteine protease family are a good candidate as they play essential roles in tumor growth, angiogenesis, resistance to apoptosis, and invasion.[12, 13] A member of this family, cathepsin B, is commonly active in the tumor microenvironment in various human cancers including breast cancer.[12, 14-16] Upregulated expression of cathepsin B is found in tumor, endothelial and immune cells, in particular macrophages.[13] Cathepsin B overexpression in human breast carcinomas is associated with poor differentiation, lymph node involvement, absence of estrogen receptor expression and impaired overall survival.[17, 18]

The protease-activatable NIR fluorescence probe ProSense (VisEn Medical, Woburn, USA) has been shown to detect a variety of tumors in nude or transgenic mice.[19-31] However, as tumor progression and metastasis are regulated by the surrounding microenvironment, it is important to use syngeneic animal models

that allow appropriate crosstalk at the invasive tumor border to study probes that are activated by proteolytic activity. Moreover, the use of a larger animal model such as the rat offers more challenges in terms of tissue penetration of NIR fluorescence probes.

Therefore, the aim of this study was to assess the technique of NIR fluorescence imaging in a syngeneic breast cancer rat model using ProSense and to determine the accuracy of intraoperative tumor detection to obtain an adequate tumor-free resection margin.

MATERIAL AND METHODS

Breast cancer cell line and culture conditions

The MCR86 cell line is a rapidly growing, syngeneic breast cancer cell line derived after subcutaneous transplantation of macroscopic lung tumors, which developed in a female WAG/Rij rat after intravenous inoculation of MCR83 breast cancer cells.[32] Tumor cells were cultured in RPMI 1640 supplemented with 2 mM L-glutamine (Gibco, Invitrogen Ltd, Carlsbad, USA), 10% heat-inactivated fetal calf serum, 100 U/ml penicillin and 0.1 mg/ml streptomycin sulphate.

Breast cancer model and tumor induction

The related EMR86 model is a transplantable, hormone-dependent, metastasizing mammary carcinoma that originated in a female WAG/Rij rat bearing a subcutaneously implanted estrogen pellet and is developed by our research group (Figure 1A).[33] Tumors are only induced and maintained in rats carrying estrogen pellets, whereas tumors transplanted into non-estrogenized animals do not grow out. Removal of the estrogen pellet induces apoptosis and tumor regression (Figure 1B). EMR86 tumors are histologically classified as high-grade invasive ductaltype adenocarcinomas, with both a cribiform and a solid growth pattern. In large tumors areas, comedo type necrosis can be appreciated. Tumors have a stromal compartment of approximately 30% depending on tumor size (Figure 1C). EMR86 tumor cells show strong nuclear expression of the estrogen and progesterone receptor in more than 90% of cells, but stain negative for HER2/neu receptor (Figure 1D-F). Therefore, EMR86 tumors closely resemble the luminal A molecular subtype – the most prevalent subtype of human breast cancer.[34, 35]

For tumor induction, fresh EMR86 tumor fragments of 0.5-1 mm³ were implanted in the mammary fat pad at four sites of female WAG/Rij rats (Charles River, Maastricht, the Netherlands) aging 4-6 months. (A stable cell line from EMR86 tumor has not yet been successfully established, therefore, tumor transplantation is used.) During the same session, an estrogen pellet was implanted subcutaneously in

the intrascapular region of the neck. The in-house generated pellets consist of 2 mm by 3 mm silicone tubes containing 1.5 mg 17 β-estradiol on a 1:3 cholesterol/paraffin basis. Tumor volumes were estimated twice weekly using digital calipers by measuring three orthogonal diameters of the tumor and multiplying this product by π/6. All rats were housed in the animal facility of the Leiden University Medical Center. Pellet food and fresh tap water were provided ad libitum. The weight of the animals was followed throughout the experiment to monitor their general health state. The Animal Welfare Committee of the Leiden University Medical Center approved the study. The study was conducted in concordance with the "Guidelines for the Welfare of Animals in Experimental Neoplasia" (Second Edition, 1997) available online at http://www.ncrn. org.uk/csg/animal_guides_text.pdf.
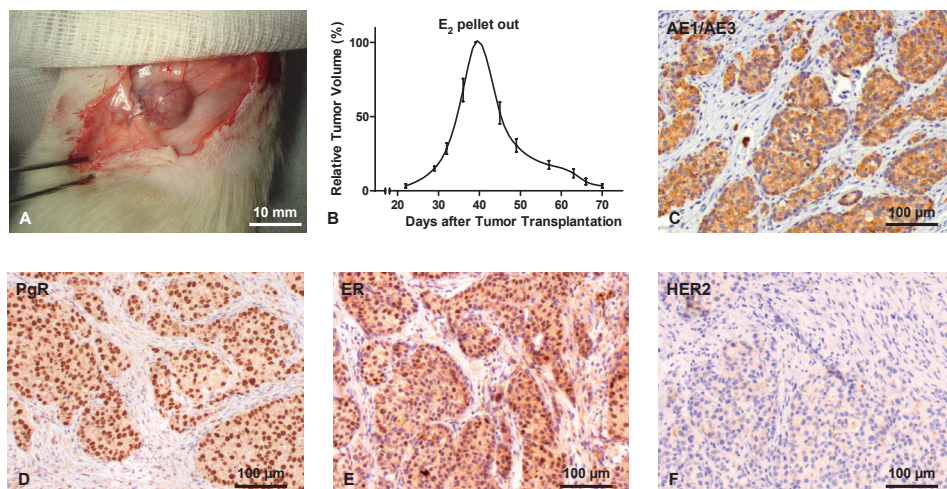

Figure 1. Description of a syngeneic rat model of hormone-dependent breast cancer. A. EMR86 breast tumors originate after transplantation of 0.5 mm3 fresh tumor fragments at the mammary fat path of female WAG/Rij rats. Shown is a tumor four weeks after transplantation. B. EMR86 tumors are only induced and maintained in rats carrying estrogen pellets. Removal of the estrogen pellet induces apoptosis and tumor regression (N = 16 tumors, 4 rats). C. EMR86 tumors are histologically classified as high-grade invasive ductal carcinomas, with both a cribiform and a solid growth pattern. Tumors have a stromal compartment of approximately 30% depending on tumor size. D-F. EMR86 tumor cells show strong nuclear expression of the estrogen and progesterone receptor in more than 90% of cells, but stain negative for HER2/neu receptor. Therefore, EMR86 tumors closely resemble the luminal A molecular subtype.

NIR fluorescence probe

The commercially available, protease-activatable NIR fluorescence probes ProSense680 and ProSense750 were used (VisEn Medical). The probes consist of a synthetic graft polymer composed of poly-L-lysine that is sterically protected by multiple methoxypolyethylene glycol side chains and to which multiple fluorophores are attached.[19] In this non-activated state, the fluorophores are positioned in close proximity to one another, which results in mutual energy transfer and thus inhibition of fluorescence emission. After enzymatic cleavage of the backbone, the fluorophores

are released and regain their fluorescent characteristics. A number of cysteine proteases are involved in this process. Cathepsin B, and to a lesser degree cathepsin K, L, and S, has been demonstrated to be a major contributor to cleavage and activation of ProSense.[19] ProSense680 and ProSense750 have peak absorption of 680 nm and 750 nm, respectively. ProSense680 was selected for intraoperative studies and fluorescence microscopy because of the better matching of the laser of the intraoperative camera system with the peak excitation of ProSense680. ProSense750 was used for cell line experiments and non-invasive animal experiments because of the better spectral separation of autofluorescence signal.

Intraoperative NIR fluorescence camera system

The Fluobeam intraoperative NIR fluorescence camera system (Fluoptics, Grenoble, France) used in this study has been described previously by our group.[36, 37] Briefly, the system is composed of a class 3B laser (100 mW) emitting at 690 nm resulting in an illumination power of 2.6 mW/cm². Filtered white light (350-650 nm) provides an irradiance of $7x10^3$ lx at the focus level. The emitted fluorescence is collected through a high pass filter (> 700 nm) by a 12 bits CCD camera resulting in a system spatial resolution of 0.17 mm/pixel.

Experimental design

Cell line experiments

For fluorescence measurements, tumor cells were harvested with a solution of 0.25% (w/v) EDTA and 0.25% (w/v) trypsin in Hanks' Buffered Salt Solution (Sigma-Aldrich, St. Louis, USA), washed three times in 0.9% phosphate buffered saline and 200 μL complete medium suspensions were made and transferred on a 96-well acrylate plate (Greiner Bio-one, Alphen aan de Rijn, the Netherlands, #655090; suitable for fluorescence measurements) and kept at 37 °C and 5% CO_2. At day 2, cells were washed and autoquenched ProSense750 (22.5 to 180 nM, 200 μl) was added. At day 3, cells were washed and 200 μl complete medium was added. Also, time-dependent studies were performed, during which ProSense750 was added at the indicated time-points (8 to 48 h). Fluorescence intensity was measured using the Odyssey NIR fluorescence scanning device (LI-COR Biosciences, Lincoln, USA). Overlying grids were drawn and fluorescence intensity was measured for each well using the Odyssey software (Version 2.1).

Animal experiments

Throughout injection, imaging and surgical procedures, rats were anaesthetized with inhalation of 2% mixture of isoflurane in oxygen. The rats were constantly monitored for the rate of the respiration and depth of anesthesia. Before imaging, rats were shaved to reduce absorption of the optical signal. A total of 20 rats bearing 77 primary mammary tumors varying in size from 0.01 to 1.8 cm^3 were used in this study.

In a dose- and time-dependent experiment, tumor-bearing rats (N = 9) were randomly assigned over three ProSense750 dose groups and intravenously injected with 2.5, 5 or 10 nmol ProSense750 (150 μl). Whole-body fluorescence was measured 24 h and 48 h after administration of ProSense750 using the IVIS Spectrum (Caliper LifeSciences, Hopkinton, USA), which allowed separation of the ProSense750 signal from the background fluorescence by means of spectral unmixing.[38] Acquisition settings were kept constant for the different dose groups and on the two consecutive days. Total photon counts per second were measured for each tumor using the Living Image software (Version 3.0, Caliper LifeSciences) and divided by the tumor volume as assessed by digital caliper measurement.

In an intraoperative experiment, tumor-bearing rats (N = 7) were operated under direct fluorescence guidance 24 h after intravenous administration of 10 nmol ProSense680 (150 μl). NIR fluorescence intensity of exposed tumors and surrounding tissues was measured with the Fluobeam intraoperative camera system. Tumor-to-background ratios were calculated by drawing regions of interest at the tumor and at the surrounding tissue by visual interpretation and subsequent measurement of fluorescent intensity using the open-source software ImageJ.[39] Merged visible light and NIR fluorescence light images were created using Adobe Photoshop CS3 Software (Version 10.0.1, Adobe Systems Inc., San Jose, USA). In order to determine sensitivity and specificity of the intraoperative NIR fluorescence technique, an attempt was made to completely remove all tumor tissue while removing as little as possible of the normal surrounding mammary fat pad tissue strictly based on the fluorescence signal in 5 of these 7 rats. Tumors were removed by sharp dissection. Excised tumors were inked with India ink, sliced in two or three parts depending on the size of the tumor and fixed overnight in 4% buffered formalin and embedded in paraffin (FFPE) blocks, mimicking the standard clinical workflow. After resection of the primary tumor, the surgical cavity was inspected with the Fluobeam to detect any remnant fluorescent tissue. After resection of all remnant fluorescent spots, random biopsies were taken of the surgical cavity from every quadrant in order to determine specificity of the technique. In one additional rat an irradical resection was performed intentionally to test the Fluobeam's ability to detect remnant tumor tissue. All specimens were fixed in formalin as described above. FFPE tumor sections of 4 μm were air-dried and stained with hematoxylin and eosin (H&E). The tumor size, the minimum and maximum

tumor-free margin and the presence of tumor in the random biopsies were determined by an experienced breast pathologist (V.T.H.B.M.S.).

Fluorescence microscopy

Cell line experiments

Time-dependent microscopic analysis of ProSense680 activation by cultured MCR86 cancer cells was performed using the LSM510 Zeiss confocal microscope (Jena, Germany, 40x/0,75w Ph2 ACHROPLAN objective). A 633 nm laser was used for fluorescence excitation and a 650 nm Long Pass for emission. Cells were cultured in 3.5 cm petri dishes incubated with 33.3 nM ProSense680 in 3 ml medium. Cells were kept at 37 °C and imaged for 4.5 hours.

Ex vivo tumor imaging

Freshly excised tumors with a wide rim of surrounding normal mammary tissue of rats injected with 10 nmol ProSense680 (N = 3) were halved. From one half, a 2 mm section was analyzed using the Odyssey scanning device at 21 μm resolution. Tumor border was defined as the outer rim of the tumor and its width was approximately 15% of the tumor diameter. The other half was snap-frozen on dry ice and stored at -80 °C. Unfixed 20 μm sections were measured for fluorescence using the Odyssey scanning device at 21 μm resolution. Processing of sections was performed under reduced light conditions to prevent photobleaching. Subsequently, the tissue sections were stained with H&E. The fluorescence image and the H&E image were merged using Adobe Photoshop enabling detailed analysis of the NIR fluorescence distribution along with the histological context.

Statistical analysis

Statistical analyses and generation of graphs were performed using GraphPad Prism software (Version 5.01, La Jolla, USA). Continuous variables were analyzed using the (paired) t-test for comparison of two groups and one-way analysis of variance (ANOVA) for comparison of more than two groups. To test the effect of two independent variables two-way ANOVA was used. Trend analysis and one-tailed planned comparisons between adjacent groups were conducted. When the assumption of homogeneity of variance was violated (Levene's test), the Brown-Forsythe F-ratio was reported. Pearson's correlation coefficients R were calculated for correlation analyses. All statistical tests were two-tailed and $P < .05$ was considered significant.

RESULTS

In vitro activation of ProSense by breast cancer rat cell line

The autoquenched NIR fluorescence probe ProSense680 was activated by MCR86 breast cancer cells within two hours. Microscopic analysis revealed an intracellular localization of activated ProSense680 (Figure 2A-B). Both incubation time ($F(3, 36)$ = 1615, $P < .0001$) and concentration of ProSense750 ($F(3, 36)$ = 3704, $P < .0001$) significantly influenced ProSense750 activation as measured by fluorescence intensity (two-way ANOVA, Fig. 2C). Also, there was an interaction between incubation time and ProSense750 concentration ($F(9, 36)$ = 230.4, $P < .0001$), indicating that the difference in incubation time within ProSense750 concentration groups influenced ProSense750 activation. Furthermore, fluorescence intensity was highly correlated with number of MCR86 cells ($F(4, 10.97)$ = 39.13, $P < .0001$, $R = 0.904$; Figure 2D).
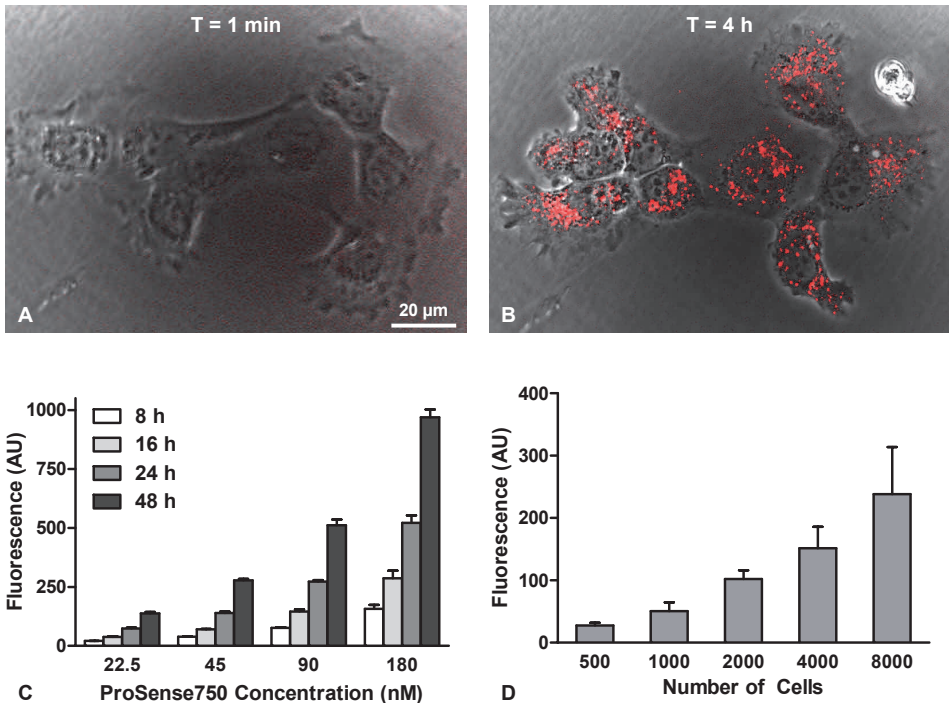

Figure 2. *In vitro* activation of ProSense by syngeneic breast cancer rat cell line. A,B. Fluorescence microscopy (LSM510 Zeiss confocal microscope, 40x objective) of a cluster of MCR86 cells, 1 minute (left panel) and 4.5 h (right panel) after incubation with ProSense680 (33.3 nM). **C.** ProSense750 concentration and incubation time both significantly influence NIR fluorescence intensity (4.000 MCR86 cells per well, two-way ANOVA, Odyssey scanner). Bars represent mean ± SEM (N = 4). **D.** NIR fluorescence intensity is positively correlated with number of MCR86 cells (45 nM ProSense750, 24 h incubation, $R = 0.890$, $P < .0001$, Odyssey scanner). Bars represent mean ± SEM (N = 8).

In vivo **activation of ProSense by syngeneic rat model of primary breast cancer**

EMR86 breast tumors were successfully imaged percutaneously using the IVIS Spectrum after intravenous administration of ProSense750 (Figure 3A-B). To test the effect of ProSense750 dose and time of imaging on fluorescence intensity, nine rats (N = 35 mammary tumors, mean volume = 0.38 ± 0.36 cm³) were randomly assigned to three ProSense750 dose groups and were imaged 24 h and 48 h post-injection. In concordance with the *in vitro* data, ProSense750 dose significantly influenced fluorescence intensity ($F(2,32) = 3.56$, $P = .04$, two-way ANOVA, Figure 3C). Of note, a substantial part of the tumors could not be identified in the 2.5 nmol dose group (24 h: 4 of 11 tumors, 48 h: 7 of 11 tumors) and the 5 nmol dose group (24 h: 2 of 12 tumors, 48 h: 3 of 12 tumors), whereas in the 10 nmol dose group all tumors were identified. In contrast to the *in vitro* data, time of imaging did not influence fluorescence intensity ($F(2,32) = 2.47$, $P = .13$, two-way ANOVA, Figure 3C). Furthermore, there was no interaction between time of imaging and ProSense750 dose ($F(2,32) = 1.06$, $P = .36$), indicating that the difference in time of imaging within dose groups did not influence fluorescence intensity. Based on these results, a dose of 10 nmol was selected for further *in vivo* testing. Imaging 24 h after ProSense administration was selected for practical purposes. With these settings, fluorescence intensity was significantly correlated with tumor volume ($R = 0.93$, $P < .0001$; Figure 3D), which was in concordance with the *in vitro* data.

Intraoperative NIR fluorescence-guided resection of primary breast cancer

Using the Fluobeam intraoperative camera system, all primary breast tumors (N = 26 tumors, 7 rats) were successfully identified 24 h after intravenous administration of 10 nmol ProSense680 (Figure 4A). The technique provided a clear demarcation of tumor and surrounding mammary fat pad tissue with a mean tumor-to-background ratio of 2.35 ± 0.37 (paired $t = 14.95$, $P < .0001$, Figure 4B). To determine the accuracy of tumor margin detection of the intraoperative NIR fluorescence technique, 17 tumors (N = 5 rats) were resected completely under direct, real-time NIR fluorescence guidance, while removing as little as possible of the normal surrounding mammary fat pad tissue and processed for histopathological analysis (Figure 4C). All 17 tumors were completely excised with a mean minimum and a mean maximum tumor-free margin of 0.2 ± 0.2 mm and 1.3 ± 0.6 mm, respectively (Table 1). Mean pathological tumor size was 5.0 ± 2.1 mm. In two cases, after resection of the primary tumor, remnant fluorescent tissue was detected in the surgical cavity with the Fluobeam (Table 1). One specimen contained a lymph node with metastatic involvement and the other contained a reactive lymph node with abundant macrophage influx but no tumor involvement. This false-positive finding can be explained by the fact that macrophages show high cathepsin B expression.[13] After resection of all fluorescent spots, random biopsies were taken of the surgical cavity from every quadrant. None of the random
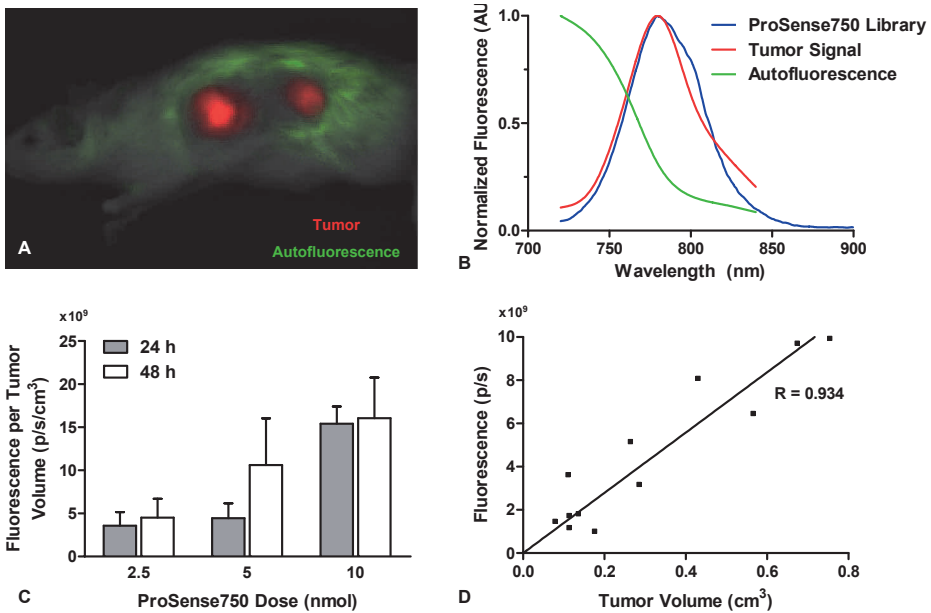
Figure 3. *In vivo* **activation of ProSense by syngeneic rat model of primary breast cancer. A.** Typical example of a spectral unmixed image of an EMR86 tumor-bearing female WAG/Rij rat, acquired 24 h after intravenous administration of 10 nmol ProSense750. Shown is the separation of the autofluorescence signal (pseudocolored green) and the ProSense750 signal (pseudocolored red; IVIS Spectrum). **B.** Emission curve plot of the spectrally unmixed fluorescence signals from **A.** demonstrates matching of the tumor signal (red line) with the predefined ProSense750 emission curve (blue line), confirming the localization of activated ProSense750 at the tumors. **C.** In a dose- and time-dependent experiment, nine tumor-bearing rats (N = 35 tumors) were randomized to three ProSense750 dose groups and imaged 24 h (grey bars) and 48 h (open bars) after intravenous administration of ProSense750 using the IVIS Spectrum. Bars represent mean ± SEM. **D.** Scatter plot of fluorescence intensity and tumor volume of the 10 nmol dose group imaged 24 h after intravenous administration of ProSense750 (R = 0.934, P < .0001, N = 12 tumors from 3 rats).

biopsies (N = 64, 5 rats) contained histologically any tumor cells. These results indicate an excellent accuracy of the technique. In one additional rat, an irradical resection was performed intentionally in order to show the Fluobeam's ability to detect remnant tumor tissue (Supplementary Figure 1). Remnant tumor tissue could be detected and subsequently resected under direct NIR fluorescence guidance.

Ex vivo NIR fluorescence microscopy

In order to determine the histological localization of ProSense680, tumors were excised with a wide rim of normal mammary tissue 24 h after intravenous administration of 10 nmol ProSense680 (N = 12 tumors, 3 rats; Figure 5A). Fluorescence imaging of 2 mm thick, fresh tumor slices revealed that the NIR fluorescence intensity was 1.6 ± 0.3 times higher at the border of the tumor than at its center (paired t = 4.99, P = .0005, N = 12 tumors; Figure 5B). In order to obtain more detail about the histological localization of ProSense680, unfixed 20 μm frozen tissue sections were measured for

Table 1. Pathological assessment of inked resection margins after NIR fluorescence guided excision of primary breast cancer

Rat	Tumor ID	Maximum ø Specimen (mm)	Maximum ø Tumor (mm)	Radical resection?	Minimum margin (mm)	Maximum margin (mm)	Remnant fluorescence tumor-positive?	Random non-fluorescence biopsies tumor-positive?
A	1	7.4	3.8	yes	<0.1	1.3	0	0/4
	2	2.8	0.8	yes	<0.1	0.9	1/1[a]	0/4
	3	8.8	4.8	yes	0.7	2.4	0	0/3
B	4	7.5	5.1	yes	<0.1	1.4	0	0/4
	5	4.9	3.1	yes	<0.1	1.0	0	0/4
	6	5.4	4.2	yes	0.1	1.0	0	0/4
	7	9.2	8.0	yes	<0.1	1.0	0	0/4
C	8	9.1	7.9	yes	<0.1	1.1	0	0/4
	9	8.9	5.7	yes	0.2	2.5	0	0/4
	10	9.7	7.7	yes	<0.1	1.8	0	0/4
D	11	5.3	2.4	yes	0.4	1.6	0	0/3
	12	6.1	4.3	yes	0.2	1.0	0	0/4
	13	5.7	4.4	yes	0.2	1.5	0	0/4
E	14	8.2	6.9	yes	<0.1	0.8	0	0/4
	15	8.3	7.3	yes	<0.1	0.6	0	0/4
	16	7.3	5.6	yes	0.3	0.7	0	0/4
	17	6.6	3.0	yes	<0.1	1.9	0/1[b]	0/4
Mean ± SD		**7.1 ± 1.9**	**5.0 ± 2.1**		0.2 ± 0.2	1.3 ± 0.6	1/2	0/64

[a] Macrometastasis in lymph node
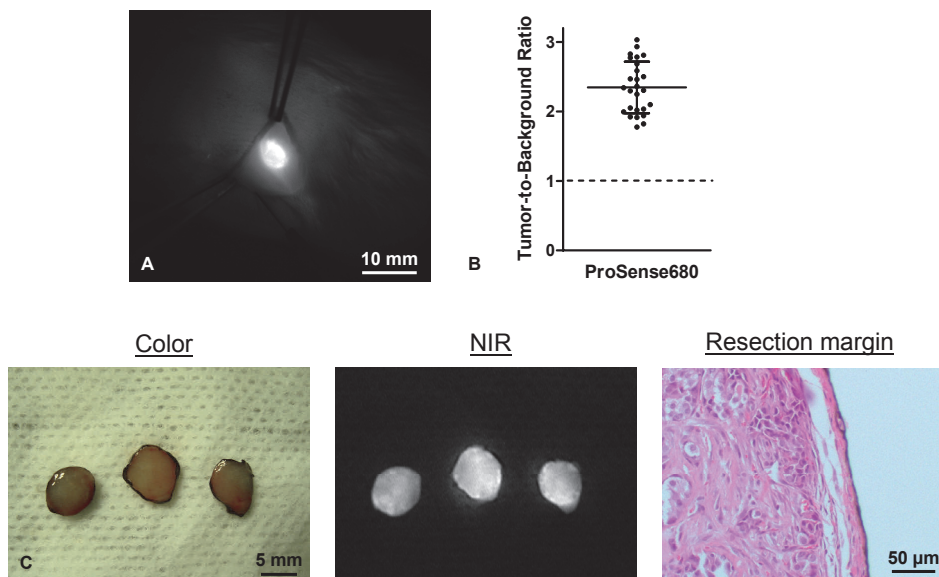[b] Reactive lymph node with abundant macrophage influx

Figure 4. Intraoperative NIR fluorescence-guided resection of primary breast cancer and pathological assessment. **A.** Intraoperative NIR fluorescence image showing a 6-mm EMR86 breast tumor in a female WAG/Rij rat 24 h after intravenous administration of 10 nmol ProSense680 (Fluobeam camera system). Camera exposure time was 10 ms. **B.** Tumor-to-background ratios were determined *in vivo* in rats 24 h after intravenous administration of 10 nmol ProSense680 (N = 26 tumors, 7 rats). Fluobeam camera exposure time was 10 ms. Horizontal lines represent mean ± SD. Mean tumor-to-background ratio was 2.35 ± 0.37. **C.** *Ex vivo* color image (left panel), NIR fluorescence image (Fluobeam, middle panel) of 3 slices of an EMR86 tumor after resection and inking using India ink. The tumor was excised from a rat 24 h after intravenous administration of 10 nmol ProSense680. Camera exposure time was 10 ms. Resection margin of the tumor is shown after H&E staining of a 4 µm FFPE tissue section (right panel).

fluorescence using the Odyssey and subsequently stained with H&E (Figure 5C). These results showed that NIR fluorescence is mainly located in the stromal compartment of the breast tumors and in particular at the tumor border.

DISCUSSION

In the current study, we demonstrated the feasibility of real-time intraoperative NIR fluorescence identification of breast tumors in a syngeneic orthotopic breast cancer rat model using the protease-activatable probe ProSense. In both the cell line and animal experiments, fluorescence intensity was strongly correlated with number of tumor cells, tumor size and ProSense dose. In contrast to the *in vitro* data, time of imaging (24 h vs. 48 h after administration of ProSense) did not significantly influence fluorescence intensity of breast tumors. This is likely a result of the relatively long blood half-life of ProSense (half-life in mice 18 h, VisEn Medical website) and may provide flexible operation planning in future clinical applications. Histological analysis demonstrated that NIR fluorescence intensity of tumors was highest at the invasive tumor border.

Resection of tumors under real-time NIR fluorescence guidance showed excellent accuracy of the technique in the intraoperative detection of tumor margins. These results suggest that clinical introduction of intraoperative NIR fluorescence imaging using a protease-activatable probe such as ProSense has the potential to increase the number of complete tumor resections in breast cancer patients undergoing breast-conserving surgery.

Previous studies in which NIR fluorescent and protease-activatable probes were tested have utilized xenograft or transgenic mouse models.[19-31] A limitation of many animal models of breast cancer is that, compared to the human situation, less normal mammary tissue is present in relation to tumor size. Therefore, these tumors are easily resected by removing all breast tissue. However, this approach does not resemble the principles underlying breast-conserving surgery. This study was performed using an orthotopic breast cancer model that is syngeneic to immunocompetent female WAG/Rij rats. In syngeneic models, tumors are grown in homologous species and in the strain in which the tumor has originated. Therefore, these models are more representative of the natural tumor-host interaction. Although no preclinical tumor model will contain all features of the complex biology of human cancer, this syngeneic model has several strengths, including its hormone-sensitivity, cribiform growth pattern and its ability to induce regression by estrogen pellet removal. Moreover, this model captures several important features of luminal A hormone-dependent, HER2/neu negative human breast cancer, which is the most predominant subtype of breast cancer.[34, 35] Another intrinsic limitation of animal models of surgical interventions is the potential occurrence of performance bias, because researchers carrying out the intervention can not be blinded to the allocated treatment. This form of bias may lead to flawed results.[40] To surpass these limitations in our study, a one-arm study design was chosen using small breast tumors (5.0 ± 2.1 mm). Tumors were excised based on the NIR fluorescence signal and examined by a breast pathologist using standard clinical methodology. Using this approach, all tumors were completely resected with a mean maximum tumor-free resection margin of 1.3 ± 0.6 mm, indicating that a minimal amount of normal mammary tissue was resected. Although syngeneic models provide a relevant tumor-host interaction, their major drawback is that the tumor cells are rodent, and therefore express the rodent homologues of the desired targets. However, the main target of ProSense, the cysteine protease family (most particular cathepsin B) is strongly conserved amongst mammals.[12] Upregulation of cathepsin B has been confirmed extensively in human breast cancer.[12, 14, 15, 41] It is therefore expected that this kind of protease-activated NIR fluorescence probes will be applicable for intraoperative NIR fluorescence imaging in a large proportion of breast cancer patients.

Analysis of the histological localization of activated ProSense demonstrated that the invasive tumor border exhibited the most intense NIR fluorescence signal. This observation is in concordance with immunohistological analysis of cathepsin B
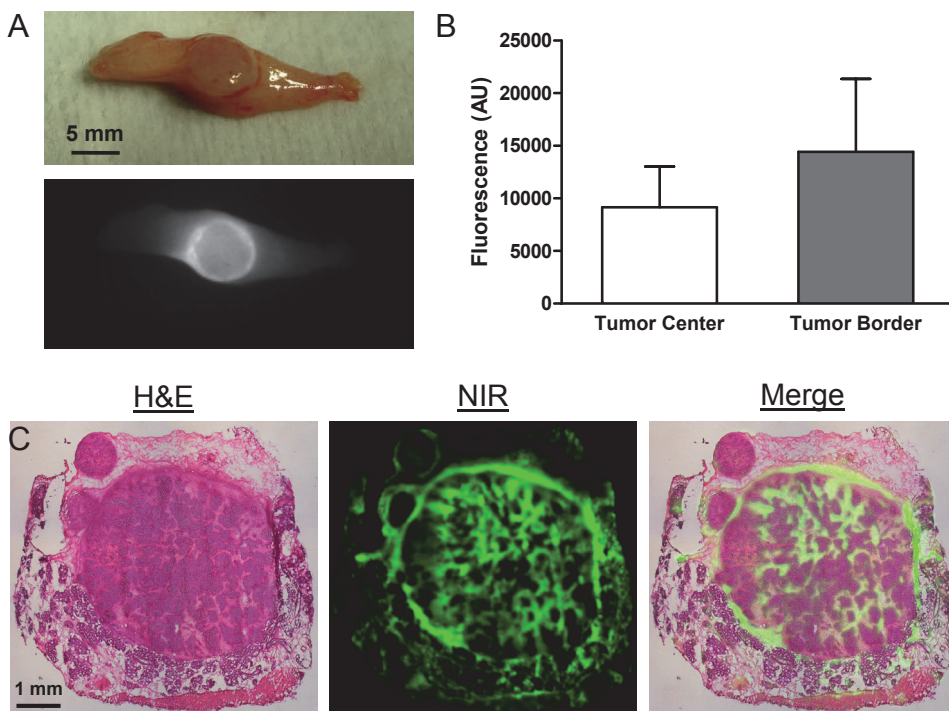
Figure 5. *Ex vivo* **NIR fluorescence microscopy of resected breast cancer. A.** *Ex vivo* color image (top panel) and NIR fluorescence image (Fluobeam, bottom panel) of an excised EMR86 tumor with surrounding normal mammary fat pad. Fluobeam camera exposure time was 10 ms. The tumor was excised from a rat 24 h after administration of 10 nmol ProSense680. **B.** Quantification of NIR fluorescence measurements of tumor tissue slices showed that the fluorescence signal was 1.6 ± 0.3 times higher at the border of the tumor than at its center (Odyssey scanner, paired $t = 4.99$, $P = .0005$, N = 12 tumors). **C.** Shown are a color image of H&E staining (left panel), a pseudocolored green NIR fluorescence image (middle panel; Odyssey scanner), and a merge of the two images (right panel) of a 20 µm frozen section of a 4-mm EMR86 breast tumor with surrounding mammary fat pad. The tumor was excised from a rat 24 h after administration of 10 nmol ProSense680.

reported by others[14, 24] and is in line with the pathophysiological role of cathepsins as reviewed by Gocheva.[42] Cathepsins promote tumor invasion through several possible mechanisms. First, they can directly cleave components of the extracellular matrix and basement membrane, essentially clearing a path for the migration of tumor cells away from the primary tumor. Second, at the cell membrane, cathepsins can direct a proteolytic cascade in which they activate other proteases such as matrix metalloproteinases and urokinase plasminogen activator, which in turn promotes tumor invasion. Third, cleavage of the cell adhesion protein, E-cadherin, at the cell surface can disrupt adherens junctions and thus facilitate cancer cell migration and invasion.[42] Apart from tumor border, NIR fluorescence was higher in the stromal compartment of the tumors. This finding is in concordance with Gounaris et al., who demonstrated that CD11+ tumor-infiltrating macrophages accounted for 75% of the ProSense signal at FACS analysis.[29] In summary, as complete resection of breast tumors

requires adequate visualization of tumor margins, the increased activity of proteolytic enzymes at the invasive tumor border provides an excellent target for intraoperative NIR fluorescence-guided surgery.

Future clinical studies will have to provide proof-of-principle of intraoperative NIR fluorescence tumor detection. Currently, a number of intraoperative NIR fluorescence imaging systems are clinically available and have already been used for sentinel lymph node mapping.[43-45] It is expected that several tumor-targeting NIR fluorescent probes (such as ProSense) will receive regulatory approval within the next few years.

A therapeutic challenge of any new breast cancer imaging technology is the detection of occult tumor deposits in the breast. These tumor deposits could influence surgical decision making, but do not necessarily have a prognostic relevance, because postoperative radiation will eradicate these microscopic deposits in the vast majority of cases. For instance, in preoperative magnetic resonance imaging, the identification of additional tumor deposits is two to three times higher than the incidence of local recurrence, resulting in mastectomies that may not be beneficial to the patient.[46] Consequently, detection of tumor at the margins would be beneficial; detection of tumor deposits beyond the margins, below the cut edge of the lumpectomy cavity, could have the potential to increase surgical resection volume (or even mastectomy rates) without a benefit in survival. Since the maximum penetration depth for NIR fluorescence imaging is currently around 1 cm,[47] it is unlikely that intraoperative NIR fluorescence imaging will detect occult lesions at several centimeters distance from the primary tumor.

Sensitivity of NIR fluorescence is mostly dependent on photon absorption of the tissue, fluorescence excitation power of the light source and concentration of the NIR fluorophore in tissue. Required camera exposure times are inversely correlated with the amount of fluorescence signal. In the current study, camera exposure times of 2-20 ms were used. The field-of-view of the Fluobeam camera system is 7 cm of diameter. Therefore, the time needed to evaluate tumor margins and excision cavities is at most several seconds. Consequently, this real-time intraoperative technique is unlikely to prolong surgical time significantly.

In conclusion, this study provides preclinical validation of an innovative technique in which NIR fluorescence light is used to visualize breast tumors and to provide real-time guidance during subsequent resection. Clinical translation of these results might be very promising because of high accuracy of the technique, flexible surgical planning, increased proteolytic activity at the tumor border and upregulation of cathepsin B in a large proportion of breast cancer patients. Therefore, this study warrants clinical validation of this technique, once NIR fluorescence probes become available for clinical testing, with the ultimate goal to increase the radical resection rate of patients undergoing breast-conserving surgery.

ACKNOWLEDGEMENTS

REFERENCES

1. Mai KT, Yazdi HM, Isotalo PA. Resection margin status in lumpectomy specimens of infiltrating lobular carcinoma. Breast Cancer Res Treat 2000; 60:29-33.
2. Chagpar AB, Martin RC, Hagendoorn LJ, et al. Lumpectomy margins are affected by tumor size and histologic subtype but not by biopsy technique. Am J Surg 2004; 188:399-402.
3. Smitt MC, Horst K. Association of clinical and pathologic variables with lumpectomy surgical margin status after preoperative diagnosis or excisional biopsy of invasive breast cancer. Ann Surg Oncol 2007; 14:1040-4.
4. Rizzo M, Iyengar R, Gabram SG, et al. The effects of additional tumor cavity sampling at the time of breast-conserving surgery on final margin status, volume of resection, and pathologist workload. Ann Surg Oncol 2010; 17:228-34.
5. Hewes JC, Imkampe A, Haji A, et al. Importance of routine cavity sampling in breast conservation surgery. Br J Surg 2009; 96:47-53.
6. Clarke M, Collins R, Darby S, et al. Effects of radiotherapy and of differences in the extent of surgery for early breast cancer on local recurrence and 15-year survival: an overview of the randomised trials. Lancet 2005; 366:2087-106.
7. Nyirenda N, Farkas DL, Ramanujan VK. Preclinical evaluation of nuclear morphometry and tissue topology for breast carcinoma detection and margin assessment. Breast Cancer Res Treat 2011; 126:345-54.
8. Stepp H, Beck T, Pongratz T, et al. ALA and malignant glioma: fluorescence-guided resection and photodynamic treatment. J Environ Pathol Toxicol Oncol 2007; 26:157-64.
9. Ishizawa T, Fukushima N, Shibahara J, et al. Real-time identification of liver cancers by using indocyanine green fluorescent imaging. Cancer 2009; 115:2491-504.
10. Nguyen NQ, Biankin AV, Leong RW, et al. Real time intraoperative confocal laser microscopy-guided surgery. Ann Surg 2009; 249:735-7.
11. Frangioni JV. New technologies for human cancer imaging. J Clin Oncol 2008; 26:4012-21.
12. Mohamed MM, Sloane BF. Cysteine cathepsins: multifunctional enzymes in cancer. Nat.Rev. Cancer 2006; 6:764-75.
13. Gocheva V, Zeng W, Ke D, et al. Distinct roles for cysteine cathepsin genes in multistage tumorigenesis. Genes Dev 2006; 20:543-56.
14. Parker BS, Ciocca DR, Bidwell BN, et al. Primary tumour expression of the cysteine cathepsin inhibitor Stefin A inhibits distant metastasis in breast cancer. J Pathol 2008; 214:337-46.
15. Harbeck N, Alt U, Berger U, et al. Prognostic impact of proteolytic factors (urokinase-type plasminogen activator, plasminogen activator inhibitor 1, and cathepsins B, D, and L) in primary breast cancer reflects effects of adjuvant systemic therapy. Clin Cancer Res 2001; 7:2757-64.
16. Lah TT, Kokalj-Kunovar M, Strukelj B, et al. Stefins and lysosomal cathepsins B, L and D in human breast carcinoma. Int J Cancer 1992; 50:36-44.
17. Lah TT, Kos J, Blejec A, et al. The expression of lysosomal proteinases and their inhibitors in breast cancer: possible relationship to prognosis of the disease. Pathol Oncol Res 1997; 3:89-99.
18. Foekens JA, Kos J, Peters HA, et al. Prognostic significance of cathepsins B and L in primary human breast cancer. J Clin Oncol 1998; 16:1013-21.
19. Weissleder R, Tung CH, Mahmood U, et al. In vivo imaging of tumors with protease-activated near-infrared fluorescent probes. Nat Biotechnol 1999; 17:375-8.

20. Kirsch DG, Dinulescu DM, Miller JB, et al. A spatially and temporally restricted mouse model of soft tissue sarcoma. Nat Med 2007; 13:992-7.

21. Bremer C, Tung CH, Bogdanov A, Jr., et al. Imaging of differential protease expression in breast cancers for detection of aggressive tumor phenotypes. Radiology 2002; 222:814-8.

22. von Burstin J, Eser S, Seidler B, et al. Highly sensitive detection of early-stage pancreatic cancer by multimodal near-infrared molecular imaging in living mice. Int J Cancer 2008; 123:2138-47.

23. Sheth RA, Upadhyay R, Stangenberg L, et al. Improved detection of ovarian cancer metastases by intraoperative quantitative fluorescence protease imaging in a pre-clinical model. Gynecol Oncol 2009; 112:616-22.

24. Alencar H, Funovics MA, Figueiredo J, et al. Colonic adenocarcinomas: near-infrared microcatheter imaging of smart probes for early detection - study in mice. Radiology 2007; 244:232-8.

25. Bogdanov AA, Jr., Lin CP, Simonova M, et al. Cellular activation of the self-quenched fluorescent reporter probe in tumor microenvironment. Neoplasia. 2002; 4:228-36.

26. Niedre MJ, de Kleine RH, Aikawa E, et al. Early photon tomography allows fluorescence detection of lung carcinomas and disease progression in mice in vivo. Proc Natl Acad Sci USA 2008; 105:19126-31.

27. Ntziachristos V, Tung CH, Bremer C, et al. Fluorescence molecular tomography resolves protease activity in vivo. Nat Med 2002; 8:757-60.

28. Bremer C, Ntziachristos V, Weitkamp B, et al. Optical imaging of spontaneous breast tumors using protease sensing 'smart' optical probes. Invest Radiol 2005; 40:321-7.

29. Gounaris E, Tung CH, Restaino C, et al. Live imaging of cysteine-cathepsin activity reveals dynamics of focal inflammation, angiogenesis, and polyp growth. PLoS One. 2008; 3:e2916.

30. Grimm J, Kirsch DG, Windsor SD, et al. Use of gene expression profiling to direct in vivo molecular imaging of lung cancer. Proc Natl Acad Sci USA 2005; 102:14404-9.

31. Nguyen QT, Olson ES, Aguilera TA, et al. Surgery with molecular fluorescence imaging using activatable cell-penetrating peptides decreases residual cancer and improves survival. Proc Natl Acad Sci USA 2010; 107:4317-22.

32. van Dierendonck JH, Keijzer R, Cornelisse CJ, et al. Surgically induced cytokinetic responses in experimental rat mammary tumor models. Cancer 1991; 68:759-67.

33. Wijsman JH, Cornelisse CJ, Keijzer R, et al. A prolactin-dependent, metastasising rat mammary carcinoma as a model for endocrine-related tumour dormancy. Br J Cancer 1991; 64:463-8.

34. Sorlie T, Tibshirani R, Parker J, et al. Repeated observation of breast tumor subtypes in independent gene expression data sets. Proc Natl Acad Sci USA 2003; 100:8418-23.

35. Sihto H, Lundin J, Lehtimaki T, et al. Molecular subtypes of breast cancers detected in mammography screening and outside of screening. Clin Cancer Res 2008; 14:4103-10.

36. Mieog JS, Vahrmeijer AL, Hutteman M, et al. Novel intraoperative near-infrared fluorescence camera system for optical image-guided cancer surgery. Mol Imaging 2010; 9:223-31.

37. Keramidas M, Josserand V, Righini CA, et al. Intraoperative near-infrared image-guided surgery for peritoneal carcinomatosis in a preclinical experimental model. Br J Surg 2010; 97:737-43.

38. Mansfield JR, Hoyt C, Levenson RM. Visualization of microscopy-based spectral imaging data from multi-label tissue sections. Curr Protoc Mol Biol 2008; Chapter 14.

39. Rasband WS. ImageJ, U. S. National Institutes of Health, Bethesda, Maryland, USA, http://rsb.info.nih.gov/ij. 2009.

40. Juni P, Altman DG, Egger M. Systematic reviews in health care: Assessing the quality of controlled clinical trials. BMJ 2001; 323:42-6.

41. Kuester D, Lippert H, Roessner A, et al. The cathepsin family and their role in colorectal cancer. Pathol Res Pract 2008; 204:491-500.

42. Gocheva V, Joyce JA. Cysteine cathepsins and the cutting edge of cancer invasion. Cell Cycle 2007; 6:60-64.

43. Troyan SL, Kianzad V, Gibbs-Strauss SL, et al. The FLARE intraoperative near-infrared fluorescence imaging system: a first-in-human clinical trial in breast cancer sentinel lymph node mapping. Ann Surg Oncol 2009; 16:2943-52.

44. Hirche C, Murawa D, Mohr Z, et al. ICG fluorescence-guided sentinel node biopsy for axillary nodal staging in breast cancer. Breast Cancer Res Treat 2010; 121:373-8.

45. Kitai T, Inomoto T, Miwa M, et al. Fluorescence navigation with indocyanine green for detecting sentinel lymph nodes in breast cancer. Breast Cancer 2005; 12:211-5.
46. Bloom S, Morrow M. A clinical oncologic perspective on breast magnetic resonance imaging. Magn Reson Imaging Clin N Am 2010; 18:277-94.
47. De Grand AM, Lomnes SJ, Lee DS, et al. Tissue-like phantoms for near-infrared fluorescence imaging system assessment and the training of surgeons. J Biomed Opt. 2006; 11:014007.

SUPPLEMENTARY DATA
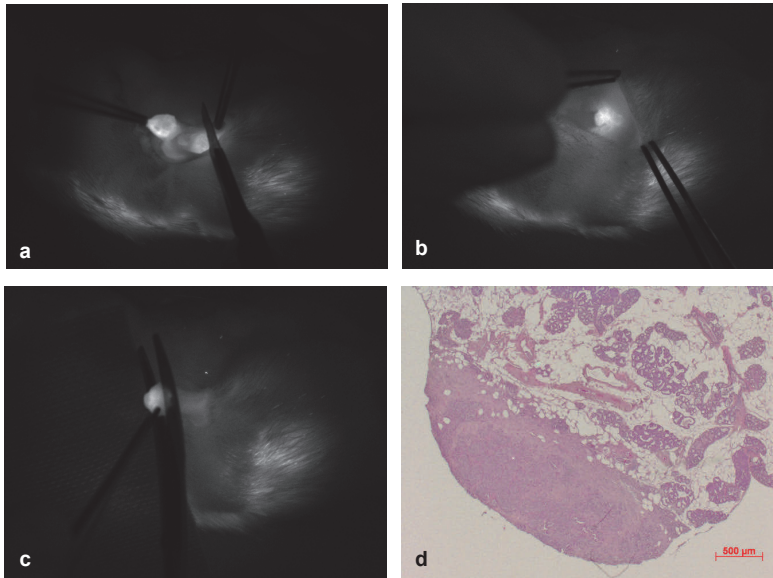
Supplementary Figure 1. Intraoperative NIR fluorescence detection of irradical resection of pirmary breast cancer. A. Intraoperative NIR fluorescence image of an intentionally irradical resection of an EMR86 tumor in a WAG/Rij rat 24 h after intravenous administration of 10 nmol ProSense680. **B.** A remnant fluorescent hotspot is readily visualized using intraoperative NIR fluorescence imaging. **C.** The identified fluorescent hotspot is resected under direct NIR fluorescence image-guidance. Camera exposure time was 10 ms. **D.** Resected hotspot is histologically confirmed as tumor tissue (H&E staining).